

Risk-Based Prioritization of a Building Portfolio for Retrofit

Hesam Talebiyan¹ and Mojtaba Mahsuli, A.M.ASCE²

Abstract: This paper puts forward a risk-based approach to prioritize a portfolio of buildings for retrofit. A new set of local sensitivity measures is proposed to rank the buildings based on the optimal mitigation of risk to the entire portfolio. The proposed measures employ the derivative of various risk measures with respect to the cost of retrofit for each building. These risk measures are the mean and higher moments of the total portfolio cost probability distribution. The total portfolio cost comprises the construction cost due to retrofit and the repair cost due to damage. The proposed sensitivity measures quantify the reduction of risk to the entire portfolio per dollar spent on retrofitting each building. They provide the flexibility to prioritize under risk-neutrality and risk-aversion. To quantify the risk, reliability methods were employed in which many interacting probabilistic models evaluate the costs. The proposed methodology was applied to prioritizing 114 masonry school buildings in Iran for seismic retrofit. To this end, models were developed to predict the repair and the retrofit cost of masonry structures. DOI: 10.1061/(ASCE)ST.1943-541X.0001927. © 2017 American Society of Civil Engineers.

Author keywords: Prioritization; Risk analysis; Local sensitivity analysis; Reliability methods; Probabilistic models; Building portfolio; Structural safety and reliability.

Introduction

Society is confronted with infinite choices to invest limited resources on improving safety. This paper addresses the problem of resource allocation to retrofitting a portfolio of buildings for optimal mitigation of the effect of hazards. In particular, it is suggested here that buildings whose retrofit yields the largest reduction of risk to the entire portfolio, per unit money spent, must be prioritized. To this end, a new set of local sensitivity measures is proposed to rank the buildings. They utilize the derivative of various risk measures with respect to the cost of retrofit for each building. The risk measures are the moments of the probability distribution of the total portfolio cost, c , obtained from a risk analysis described shortly. The total portfolio cost is the sum of two costs over all buildings: (1) Construction cost due to retrofit, denoted by c_o , which is the cost of a priori actions to enhance the performance of buildings to the desired level; and (2) repair cost due to the probable losses in the future, denoted by c_r , which is the cost of a posteriori actions undertaken in the aftermath of a hazard event to recover the buildings to undamaged, pre-event state. The first moment of c is the mean cost, $E[c]$, which reflects risk-neutral decision making in accordance with the theory of expected cost (Bernoulli 1738). In turn, the second moment, $E[c^2]$, is the mean square cost, which, together with higher moments, $E[c^n]$ where $n > 1$, reflects risk-averse decision making in accordance with the theory of expected utility (von Neumann and Morgenstern 1944). The proposed approach builds upon the work by Mahsuli and Haukaas (2013c), who employed local sensitivity analysis in portfolio prioritization for the first time.

To substantiate the metric proposed to prioritize the buildings, consider the sensitivity of the total expected cost of the entire portfolio, $E[c]$, with respect to the construction cost of the j th building in the portfolio, c_{oj} . This sensitivity measure is denoted by $\partial E[c]/\partial c_{oj}$. This measure shows the amount of change in the mean cost of the entire portfolio per unit of money spent on retrofitting the j th building. Hypothetically, if retrofit yielded no reduction in the repair cost, a unit increase in the retrofit cost of the building would result in a unit increase in the mean total cost of the entire portfolio. In reality, however, spending on retrofit results in savings due to the reduction of the repair cost. Hence, the mean portfolio cost increases less than unity per unit spent on retrofitting the building. The difference, $1 - \partial E[c]/\partial c_{oj}$, is the amount of saving due to the reduction of the repair cost. The higher this saving, the more the return of the investment on retrofitting that building. Hence, buildings with the highest $1 - \partial E[c]/\partial c_{oj}$ must be prioritized in risk-neutral decision making. This measure is dimensionless, i.e., it is in the unit of, say, dollar per dollar.

Contrary to a risk-neutral decision maker, a risk-averse decision maker tends to avoid extreme losses, which are highly uncertain. To accommodate this attitude toward risk, $E[c]$ is here replaced with $E[c^n]$, where $n > 1$, in order to weight higher costs more, i.e., to increase their effect on the decision. In fact, c^n is a concave utility function in terms of c for $n > 1$. This concavity, according to von Neumann and Morgenstern (1944), represents a risk-averse attitude toward decision making. This leads to the derivative $\partial E[c^n]/\partial c_{oj}$ to be used in a risk-averse sensitivity measure. This derivative is not dimensionless, and hence not directly comparable with $\partial E[c]/\partial c_{oj}$. To achieve such nondimensionality, the n th root of $E[c^n]$, i.e., $(E[c^n])^{1/n}$, is employed. Consequently, the sensitivity measure $1 - \partial (E[c^n])^{1/n}/\partial c_{oj}$ is proposed for decision making under risk-aversion.

To quantify the risk to the portfolio of buildings, the risk analysis approach proposed by Mahsuli and Haukaas (2013a, b) was employed. This approach yields the exceedance probabilities (EPs) of the portfolio cost, c . These probabilities are central in computing the previously mentioned sensitivity measures. In this risk analysis approach, reliability methods compute the exceedance probabilities, and many interacting probabilistic models evaluate the costs. These models simulate the occurrence and intensity of hazards as

¹M.Sc. Graduate, Dept. of Civil Engineering, Sharif Univ. of Technology, 14588-89694 Tehran, Iran. E-mail: hesam.talebiyan@rice.edu

²Assistant Professor, Dept. of Civil Engineering, Sharif Univ. of Technology, 14588-89694 Tehran, Iran (corresponding author). E-mail: mahsuli@sharif.edu

Note. This manuscript was submitted on April 22, 2016; approved on June 30, 2017; published online on November 11, 2017. Discussion period open until April 11, 2018; separate discussions must be submitted for individual papers. This paper is part of the *Journal of Structural Engineering*, © ASCE, ISSN 0733-9445.

well as the damage, repair cost, and retrofit cost of buildings. The building models were developed in this study.

The proposed prioritization methodology is showcased by a comprehensive application featuring 114 masonry school buildings in two provinces of Iran that are subject to seismicity from several sources. These buildings are ranked for seismic retrofit. For this purpose, probabilistic models that predict the repair cost and the retrofit cost of masonry buildings were developed for the conventional construction of Iran. These schools were affected by 15 sources of seismicity, each of which is modeled in this study by occurrence, magnitude, location, and intensity models.

Literature Review

Past studies proposed a number of approaches to prioritize buildings for retrofit. FEMA (1988) proposed a scoring system for this purpose, which was developed based on questionnaires filled through sidewalk surveys. Grant et al. (2007) ranked the buildings in a two-step procedure: (1) a visual inspection for vulnerability assessment that yields a short list of critical buildings; and (2) a simplified structural analysis that ranks the buildings in the short list. Tesfamariam and Saatcioglu (2008) used fuzzy logic to evaluate the seismic hazard, building vulnerability, and consequence of failure, and introduced a ranking scheme for reinforced concrete buildings. In comparison, the present study employed a local sensitivity analysis in prioritization that eliminated the need to utilize subjective information.

Monti and Nuti (1996) proposed a reliability-based methodology to identify the potential weak components of a hospital given a level of seismic hazard. The result of this analysis was used to identify the best a priori upgrading action. Nuti and Vanzi (1998) assessed the vulnerability of a hospital system and chose the best retrofit action based on minimizing the cost-benefit ratio. Using a similar approach, Nuti et al. (2004) investigated different retrofit strategies for hospitals after the 2002 Molise, Italy, earthquake, and prioritized the hospitals in the region accordingly. Vanzi (2000) identified the optimal retrofit strategy for electric power systems through minimizing the probability of cutoff at the most needed nodes in the system. These studies employed optimization-based approaches to find the best retrofit strategy.

Only a few studies have employed sensitivity analysis for prioritization. Der Kiureghian et al. (2007) prioritized the components of a system for retrofit using the derivative of a system performance measure with respect to the mean rate of failure and the mean repair duration of components. Mahsuli and Haukaas (2013c) proposed a reliability sensitivity measure for prioritization. In particular, they computed the derivative of a cost exceedance probability for all infrastructure components with respect to the cost of retrofit for each component. Bonstrom and Corotis (2015) employed the same sensitivity measure to rank buildings of a region under seismic hazard. They studied different levels of spending and considered the spatial correlation of earthquake intensity. However, the latter study disregards the uncertainty in the earthquake occurrence, magnitude, and location, although the location uncertainty, in particular, affects the ranking of buildings markedly.

The risk measure in the latter two studies is the probability of exceeding a cost threshold, $G(c_t)$, in which $G(\cdot)$ denotes the complementary cumulative distribution function, and c_t denotes a cost threshold. Recall that the risk measures here are various statistical moments of the cost probability distribution, which offer several advantages. First, whereas EPs are incoherent risk measures, the ones employed in this research were coherent risk measures (Artzner et al. 1999; Rockafellar 2007). A coherent risk measure

is capable of effectively regulating and managing risks that stakeholders face (Artzner et al. 1999). This is an appealing characteristic because the proposed prioritization methodology is, in fact, a decision support tool, intended to be used by stakeholders, here, portfolio managers, to manage the risk to their building portfolio. Second, statistical moments were computed using the entire probability distribution, while the EP of a quantile, $G(c_t)$, is only one point on the distribution. As a result, a small portion of information on cost was utilized when making a decision using a single EP. In fact, such risk measures cannot account for the full range of possible consequences. For instance, c_t in Bonstrom and Corotis (2015) and Mahsuli and Haukaas (2013c) was selected on the upper tail of the cost probability distribution, and thus represents extreme events, such as severe earthquakes. As a result, any prioritization in accordance with this risk measure neglects the low-cost segment of the probability distribution, which bears significant risk because of a high rate of occurrence. Third, the risk measure $G(c_t)$ leads to risk-averse decision making because c_t was selected on the upper tail. Hence, these measures lack the ability to prioritize buildings on a risk-neutral basis. It is argued that when the consequences of decisions are comprehensively accounted for, the expected cost, which is the risk measure that is primarily employed here, serves as the logical means of decision making. It is acknowledged, however, that when consequences like casualties, socioeconomic and environmental impacts, and decline in life quality are *not* accounted for, risk-neutral decisions shift toward a less safe design. To provide an illustration, Fig. 1 shows a schematic plot of the expected total cost against a decision variable, v . The decision variable may, for instance, represent the lateral strength of a building. The counteracting contributions of the cost of consequences like damage and the cost of retrofit make the expected total cost a convex function of the decision variable. Hence, the expected total cost has a minimum that is associated with an optimum strength, denoted by v^* . Fig. 1 demonstrates two optimal values for strength: (1) v_1^* , which represents the optimal strength when only the direct economic consequences, such as repair costs, are considered; and (2) v_2^* , which represents the optimal strength when all possible consequences are accounted for. As Fig. 1 shows, neglecting some of the consequences leads to a lower optimal strength, i.e., a less safe design. To accommodate risk-averse decision making in such conditions, this paper employs higher moments of the cost probability distribution as risk measures and studies the effect of risk aversion on prioritization.

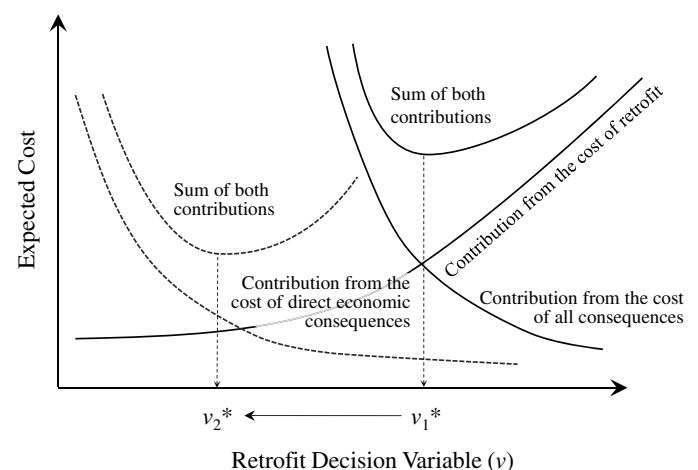


Fig. 1. Reduction of the optimal decision variable, e.g., optimal building strength, when fewer consequences are considered

Portfolio Risk Analysis

Reliability methods were employed to quantify risk. Any reliability analysis consists of two main elements: random variables and limit-state function(s). Random variables, collected in vector \mathbf{x} , describe the uncertainty in the problem, such as earthquake magnitude or model error. The limit-state function, g , describes the event the probability of which is sought. In this study, g reads

$$g(\mathbf{x}, \mathbf{v}) = c_t - c(\mathbf{x}, \mathbf{v}) = c_t - \sum_{j=1}^J c_j(\mathbf{x}, \mathbf{v}) \quad (1)$$

where \mathbf{v} = vector of decision variables, which are at the discretion of the decision maker; c_t = cost threshold; $c(\mathbf{x}, \mathbf{v})$ = total costs of the entire building portfolio; J = number of buildings; and $c_j(\mathbf{x}, \mathbf{v})$ = total cost of the j th building, which is in turn the sum of the repair cost due to damage, $c_{ij}(\mathbf{x}, \mathbf{v})$, and the construction cost due to retrofit, $c_{oj}(\mathbf{x}, \mathbf{v})$. Reliability methods compute the probability that g takes on negative values. Hence, a reliability analysis with the limit-state function in Eq. (1) computes the probability that the total costs of all J buildings exceed c_t . The construction cost of retrofit is evaluated by retrofit cost models based on the characteristics of the building as well as the type and level of retrofit. The repair cost is estimated by a chain of probabilistic models that include hazard models as well as building response, damage, and repair cost models. New models were developed for the application of this paper to predict these costs for masonry buildings. The models are presented in the "Application" section.

The first-order reliability method (FORM) (Der Kiureghian 2005) along with the load combination method (Wen 1990) were employed to compute the exceedance probability. When the chance of coincidence of hazards is negligible, a limit-state function g_i in the form of Eq. (1) for each hazard i is defined. Reliability analysis with this limit-state function yields the probability, G_i , that the total cost of all buildings exceeds the threshold c_t , given the occurrence of an event of hazard i , as follows:

$$G_i = \Phi(-\beta_i) \quad (2)$$

where Φ = standard normal cumulative distribution function; and β_i = reliability index corresponding to g_i . To compute G_i , FORM evaluates the limit-state function, g_i , and its gradient, $\partial g_i / \partial \mathbf{x}$, several times to find the design point. This point, denoted by \mathbf{x}^* , is the most probable realization of \mathbf{x} on the limit-state surface, $g_i = 0$, in the space of standard normal variables. Given the occurrence rate λ_i for hazard i , the rate of exceedance is $\lambda_i \cdot G_i$. Considering all hazards in the time period T , the load combination method computes the probability, G , that the total cost of all buildings exceeds the threshold c_t , as follows:

$$G = 1 - \exp\left(-T \cdot \sum_{i=1}^N \lambda_i \cdot G_i\right) \quad (3)$$

where N = number of hazards.

When the coincidence of two or more hazards entails a noticeable chance, additional reliability analyses are conducted for probable combinations of hazards. Given the exceedance probabilities from these reliability analyses, G is computed as

$$G = 1 - \exp\left[-T \cdot \left(\sum_{i=1}^N \lambda_i \cdot G_i + \sum_{i=1}^N \sum_{j=i+1}^N \lambda_{ij} \cdot G_{ij} + \sum_{i=1}^N \sum_{j=i+1}^N \sum_{k=j+1}^N \lambda_{ijk} \cdot G_{ijk} + \dots\right)\right] \quad (4)$$

where λ_{ij} = rate of coincidence of hazards i and j ; and G_{ij} = probability of cost exceedance under the coincidence of hazards i and j . Variables λ_{ijk} and G_{ijk} represent similar values for the coincidence of three hazards. To simplify future derivations, G is hereafter considered in the format of Eq. (3), with the exception that the dummy variable i in the said equation counts not only individual hazards, but also probable hazard combinations.

In the application that is provided in this paper, all sources of hazard are of seismic nature, i.e., they represent various sources of seismicity. Because the chance of coincident events in different seismic sources is slim, the coincidence of hazards is neglected in the "Application" section to compute G . However, it is stressed that the proposed sensitivity formulation and the prioritization methodology are capable of accounting for multiple hazards of different nature, i.e., earthquake and windstorm, but the application in this paper is seismic-oriented.

Prioritization Methodology

This study proposes the sensitivity of various moments of cost probability distribution as a means of prioritizing a portfolio of buildings for retrofit. The first moment, i.e., the expected cost, is of particular importance because it is a longstanding tenet in decision analysis and leads to risk-neutral decisions. Recall that the sensitivity of the total expected cost of the entire portfolio with respect to the construction cost of the j th building is employed to rank that building. In short, $1 - \partial E[c] / \partial c_{oj}$ serves as the metric of ranking the j th building. The generalized form of this sensitivity measure is $1 - \partial(E[c^n])^{1/n} / \partial c_{oj}$, where n is the order of the moment. In particular, $n > 1$ represents a risk-averse attitude, $n = 1$ represents a risk-neutral attitude as explained previously, and $0 < n < 1$ represents a risk-seeking attitude toward decision making. In the following, the direct differentiation method is employed to derive the formulas of computing this generalized sensitivity measure. Thereafter, the formula for the specific yet important case of $n = 1$ is derived.

To compute $\partial(E[c^n])^{1/n} / \partial c_{oj}$, the chain rule of differentiation is employed

$$\frac{\partial(E[c^n])^{1/n}}{\partial c_{oj}} = \frac{\partial(E[c^n])^{1/n}}{\partial E[c^n]} \cdot \frac{\partial E[c^n]}{\partial c_{oj}} = \frac{1}{n} \cdot (E[c^n])^{(1-n)/n} \cdot \frac{\partial E[c^n]}{\partial c_{oj}} \quad (5)$$

As a result, computation of Eq. (5) requires computing $E[c^n]$ and $\partial E[c^n] / \partial c_{oj}$. The former is the n th moment of total cost of portfolio, c , given by

$$E[c^n] = \int_0^\infty c^n f(c) dc = - \int_0^\infty c^n \frac{\partial G}{\partial c} dc \quad (6)$$

where $f(c)$ = probability density function of cost. Integrating by parts, it is extended to

$$E[c^n] = [-c^n \cdot G(c)]_0^\infty + \int_0^\infty n c^{n-1} G(c) dc \quad (7)$$

The first expression on the right-hand side is zero for $c = 0$. As c approaches infinity, the expression tends to zero because $G(c)$ decays exponentially with c for the usual cost distributions such as the one in this paper. Therefore, the first expression on the right-hand side is equal to zero, albeit for positive values of n , which is the case here. Hence, Eq. (7) is simplified to

$$E[c^n] = \int_0^\infty nc^{n-1}G(c)dc \quad \text{for } n > 0 \quad (8)$$

which is readily computed because $G(c)$ is available from the risk analysis. To compute $\partial E[c^n]/\partial c_{oj}$, which is another factor in Eq. (5), the two sides of Eq. (8) are differentiated with respect to c_{oj} as follows:

$$\begin{aligned} \frac{\partial E[c^n]}{\partial c_{oj}} &= \frac{\partial}{\partial c_{oj}} \int_0^\infty nc^{n-1}G(c)dc \\ &= \int_0^\infty n(n-1)c^{n-2} \frac{\partial c}{\partial c_{oj}} G(c)dc + \int_0^\infty nc^{n-1} \frac{\partial G(c)}{\partial c_{oj}} dc \end{aligned} \quad (9)$$

Because c is the sum of retrofit costs and repair costs, i.e., $c_{oj} + c_{lj}$, for all buildings, the term $\partial c/\partial c_{oj}$ is equal to unity. Therefore, Eq. (9) is simplified to

$$\begin{aligned} \frac{\partial}{\partial c_{oj}} \int_0^\infty nc^{n-1}G(c)dc &= \int_0^\infty n(n-1)c^{n-2}G(c)dc \\ &+ \int_0^\infty nc^{n-1} \frac{\partial G(c)}{\partial c_{oj}} dc \end{aligned} \quad (10)$$

The first term on the right-hand side may be simplified to $nE[c^{n-1}]$ for $n > 1$, which eliminates the need to compute the integral. However, without loss of generality, one may compute the first integral for $n \leq 1$.

The second integral on the right-hand side of Eq. (9) depends on the derivative of exceedance probability with respect to retrofit cost of each structure, $\partial G/\partial c_{oj}$. Using the chain rule of differentiation, $\partial G/\partial c_{oj}$ reads

$$\frac{\partial G(c)}{\partial c_{oj}} = \sum_i \left(\frac{\partial G(c)}{\partial G_i} \cdot \frac{\partial G_i}{\partial \beta_i} \cdot \frac{\partial \beta_i}{\partial v_j} \cdot \frac{\partial v_j}{\partial c_{oj}} \right) \quad (11)$$

where the dummy variable i counts hazards and probable hazard combinations; and v_j = decision variable that describes the amount of increase in lateral strength of the j th building due to retrofit. This variable is an input to both the retrofit cost model and the repair cost model. In fact, the retrofit cost increases with v . This increase is counteracted by a reduction in the repair cost. The first and second factors on the right-hand side of Eq. (11) are computed by differentiating Eqs. (2) and (3), respectively

$$\frac{\partial G_i}{\partial \beta_i} = -\varphi(\beta_i) \quad (12)$$

$$\frac{\partial G}{\partial G_i} = T \cdot \lambda_i \cdot \exp\left(-T \cdot \sum_{i=1}^N \lambda_i \cdot G_i\right) \quad (13)$$

where again the dummy variable i counts hazards and probable hazard combinations; and φ = standard normal probability density function. The third factor on the right-hand side of Eq. (11) is a well-known reliability sensitivity measure obtained by differentiating the reliability index from FORM (Der Kiureghian 2005):

$$\frac{\partial \beta_i}{\partial v_j} = \frac{1}{\|\mathbf{J}\nabla g_i\|} \cdot \frac{\partial g_i}{\partial v_j} \Big|_{\mathbf{x}^*} \quad (14)$$

where \mathbf{J} = Jacobian matrix of the probability transformation from the original space of random variables \mathbf{x} to the standard normal space. Eq. (14) is computed at the design point \mathbf{x}^* . The inverse of the fourth factor is computed by differentiating the retrofit cost

model of the j th building with respect to decision variable v_j . This model and its functional form are presented in the next section.

Finally, the derivation for ensued risk measures yields

$$\frac{\partial E[c^n]}{\partial c_{oj}} = nE[c^{n-1}] + n \int_0^\infty c^{n-1} \sum_{i=1}^N \left(\frac{\partial G(c)}{\partial G_i} \cdot \frac{\partial G_i}{\partial \beta_i} \cdot \frac{\partial \beta_i}{\partial v_j} \cdot \frac{\partial v_j}{\partial c_{oj}} \right) dc \quad (15)$$

$G(c)$ and $\partial G(c)/\partial c_{oj}$ are computed at a limited number of cost thresholds c_1, c_2, \dots, c_K , each of which requires a load combination analysis as explained previously. Hence, the integral in Eq. (15) is computed using quadrature at K points that are uniformly spaced at intervals of Δc , as follows:

$$\begin{aligned} \frac{\partial E[c^n]}{\partial c_{oj}} &= nE[c^{n-1}] + n \cdot \frac{\Delta c}{2} \left(c_1^{n-1} \cdot \frac{\partial G(c_1)}{\partial c_{oj}} \right. \\ &\quad \left. + c_K^{n-1} \cdot \frac{\partial G(c_K)}{\partial c_{oj}} + 2 \sum_{k=2}^{K-1} c_k^{n-1} \cdot \frac{\partial G(c_k)}{\partial c_{oj}} \right) \end{aligned} \quad (16)$$

The risk-neutral measure $\partial E[c]/\partial c_{oj}$, which is primarily employed in this paper, is a specific case where n is unity. In this case, the first term in Eq. (10) vanishes, and thus $\partial E[c]/\partial c_{oj}$ reads

$$\frac{\partial E[c]}{\partial c_{oj}} = \int_0^\infty \sum_{i=1}^N \left(\frac{\partial G}{\partial G_i} \cdot \frac{\partial G_i}{\partial \beta_i} \cdot \frac{\partial \beta_i}{\partial v_j} \cdot \frac{\partial v_j}{\partial c_{oj}} \right) dc \quad (17)$$

Using quadrature integration yields

$$\frac{\partial E[c]}{\partial c_{oj}} = \frac{\Delta c}{2} \left(\frac{\partial G(c_1)}{\partial c_{oj}} + \frac{\partial G(c_K)}{\partial c_{oj}} + 2 \sum_{k=2}^{K-1} \frac{\partial G(c_k)}{\partial c_{oj}} \right) \quad (18)$$

Eq. (17) essentially shows that $\partial E[c]/\partial c_{oj}$ is equal to the area underneath the $\partial G(c)/\partial c_{oj}$ curve.

Application

This section presents a comprehensive application of the proposed prioritization methodology for a portfolio of masonry buildings in Iran. Masonry construction exhibits one of the poorest seismic performances among structural systems. However, low construction cost has made such structures the majority of school buildings in developing countries. Hence, these societies are faced with a large inventory of masonry construction in need of retrofit with limited resources.

The application features a portfolio of 114 school buildings in the provinces of Qom and Markazi in central Iran that are subject to seismicity from 15 sources. Fig. 2 shows the location of these buildings with bubbles as well as the geometry of seismic sources with solid gray lines. These are the sources that fall within a radius of 200 km of the building portfolio. No active seismic sources are located on the south and the west of the portfolio within this radius.

To better show the spatial distribution of the buildings, Fig. 3 zooms in on the provinces in which the buildings are located. The numbers next to some of the locations in this figure indicate the rank of the top 10 buildings, as will be explained subsequently. To provide an overview of the information that is surveyed for this building portfolio, Table 1 presents the data for 10 example buildings. In particular, the data available for each building include footprint area, number of stories, year erected, latitude and longitude, an estimation of the mean value, type of masonry construction, type of diaphragm (flexible or rigid), and whether or not the building is

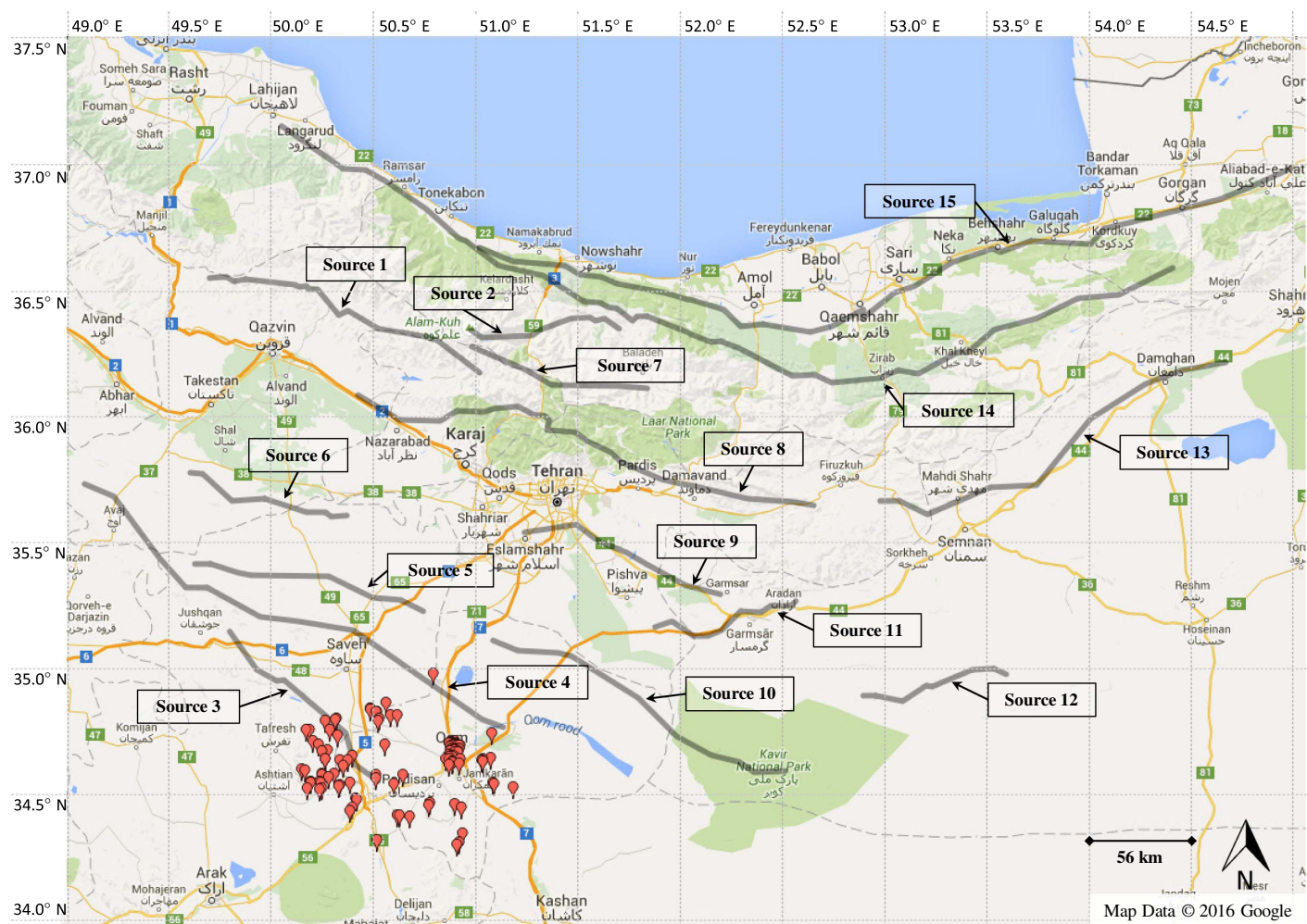


Fig. 2. Location of buildings under study and the seismic sources affecting them (map data © 2016 Google)

irregular in plan. Each building is categorized into two types of masonry construction: unreinforced masonry (URM) and confined masonry (CM). A CM structure, unlike URM, includes tie beams and tie columns in its structural system.

The prerequisite to the use of the proposed prioritization methodology for this portfolio is to quantify the seismic risk. To conduct a portfolio risk analysis with FORM, the limit-state function of Eq. (1) must be evaluated. This entails computing the seismic repair cost and retrofit cost of each building. The proposed prioritization methodology and the underlying sensitivity derivations are capable of accounting for consequences other than damage, such as casualties and downtime. For this purpose, one needs to add the costs associated with those consequences to the summation in Eq. (1). However, the scope of the application presented here is limited to repair and retrofit costs. The repair cost depends on damage, which in turn depends on the earthquake intensity, rupture location, magnitude, and occurrence. Each of these phenomena is represented by a probabilistic model. In short, a chain of probabilistic models is required to compute the limit-state function, and eventually the cost exceedance probabilities. This chain of models is illustrated in Fig. 4. For brevity, the figure shows the models for only two sources of hazards out of 15, and only two example buildings out of 114. Each box in the figure represents a probabilistic model, and the symbols that enter models by arrows are the input parameters. These parameters and their characteristics are introduced in Table 2. The parameters that enter the models from the

left are responses from upstream models, and the ones that enter from above are either random variables, decision variables, constants, or location parameters, as indicated in Table 2. Fig. 4, in fact, demonstrates the flow of information between the models. In the following section, the probabilistic models in this figure are explained in detail.

Probabilistic Models

The models in Fig. 4 may be categorized into three groups: (1) hazard models, (2) damage and repair cost models, and (3) retrofit cost models. This section addresses each of these groups, starting with hazard models. For each source of seismicity, four models were employed to make probabilistic predictions of the occurrence, location, magnitude, and intensity of seismic events within that source. The well-known Poisson point process was employed as the occurrences models, and location and magnitude models were adopted from Mahsuli and Haukaas (2013a). As for the intensity models, four ground motion prediction equations from the next-generation attenuation project (Power et al. 2008) were employed as intensity models. Given the same inputs, these equations produce different peak ground accelerations (PGAs) due to the model uncertainty. To comprehensively account for this epistemic uncertainty, the intensities that these models produce were combined by random weights, in accordance with Rahimi et al. (2015). Parameters that define the geometry,

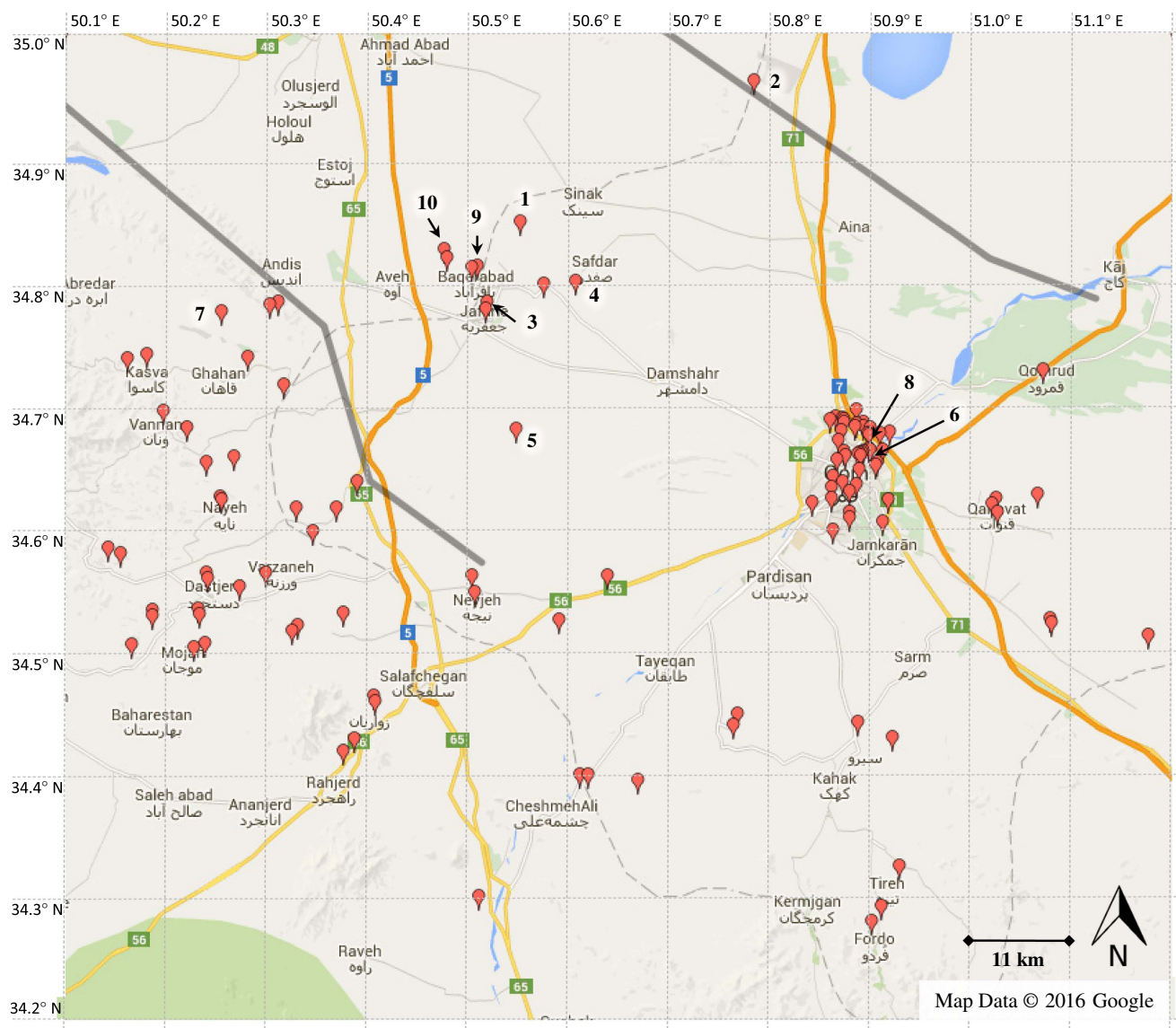


Fig. 3. Zoomed-in map of the location of 114 school buildings; the numbers on the map distinguish the top 10 prioritized buildings based on mean cost sensitivities (map data © 2016 Google)

Table 1. Information of 10 Example Buildings

Building	Latitude (°N)	Longitude (°E)	Footprint area (m ²)	Number of stories	Year erected	Mean value (dollars)	Masonry type	Plan irregularity	Diaphragm type
1	34.61	50.88	153	1	1996	152,500	URM	Yes	Rigid
2	34.62	50.88	213	1	1998	213,000	URM	Yes	Rigid
3	34.63	50.87	385	1	1985	385,000	URM	Yes	Flexible
4	34.67	50.87	580	1	1992	580,167	CM	Yes	Flexible
5	34.68	50.87	240	1	1992	240,233	CM	Yes	Flexible
6	34.60	50.88	641	2	1988	1,282,867	URM	Yes	Flexible
7	34.65	50.88	207	2	1980	413,000	CM	Yes	Flexible
8	34.63	50.89	557	2	1991	1,113,133	CM	Yes	Flexible
9	34.68	50.87	465	3	1989	1,395,000	URM	Yes	Flexible
10	34.68	50.87	450	3	1995	1,350,000	URM	Yes	Flexible

uncertainties, occurrence rate, and other characteristics of the 15 seismic sources in this study were adopted from Rahimi et al. (2015). In particular, the occurrence rate and the second moment information of the maximum magnitude, M^{\max} , and Gutenberg-Richter (Gutenberg and Richter 1944) parameter, b' , of each

seismic source are tabulated in Table 3. The source numbers are identified in Fig. 2.

Next, the Bayesian regression modeling approach (Box and Tiao 1973; Gardoni et al. 2002) was employed to develop new models for Groups 2 and 3, i.e., damage and repair cost models

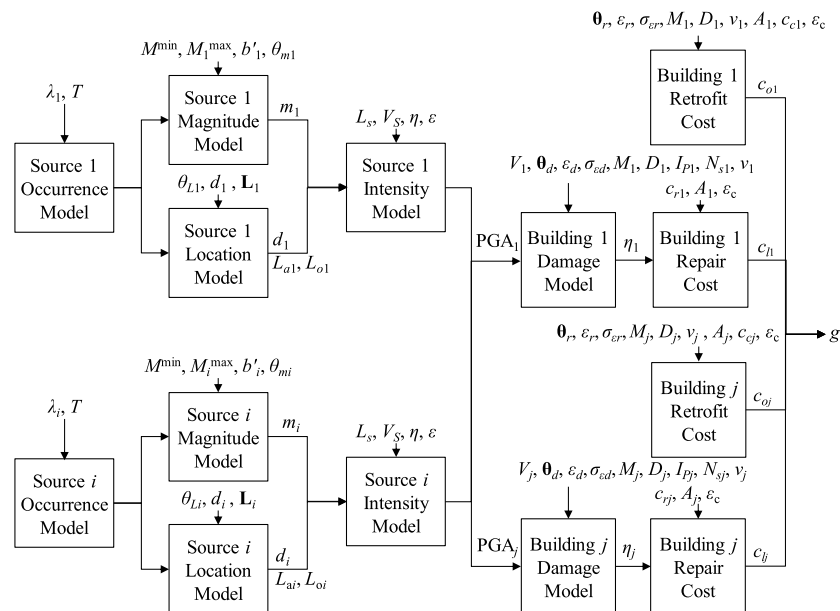


Fig. 4. Chain of models and input parameters used in the application; parameters are introduced in Table 2

Table 2. Parameters Used in the Application

Symbol	Description	Parameter type	Characteristics
A_j	Building j floor area	Constant	Varies for each building
b'_i	Source i magnitude distribution parameter	Random variable	$LN(\mu, \sigma)$ with μ and σ per Table 3
c_{ai}	Building j retrofit cost per unit area	Model response	—
c_{cj}	Building j initial construction cost per unit area	Constant	\$1,000/m ²
c_{ij}	Building j repair cost	Model response	—
c_{oj}	Building j retrofit cost	Model response	—
c_{rj}	Building j replacement cost per unit area	Constant	\$1,300/m ²
d_i	Source i depth	Model response	Dependent random variable as a function of m_i per Kaklamanos et al. (2010)
D_j	Diaphragm type of building j	Constant	Boolean, varies for each building
I_{pj}	Plan irregularity of building j	Constant	Boolean, varies for each building
L_i	Vector of source i coordinates	Location	Pairs of latitudes and longitudes
L_{ai}	Source i rupture location latitude	Model response	—
L_{oi}	Source i rupture location longitude	Model response	—
L_s	Building location	Location	Pair of latitude and longitude, varies for each building
m_i	Seismic source i magnitude	Model response	—
M_j	Masonry type of building j	Constant	Boolean, varies for each building
M_i^{\max}	Source i maximum magnitude	Random variable	User-defined distribution with moments per Table 3
M_i^{\min}	Minimum magnitude	Constant	4.8
N_{sj}	Number of stories of building j	Constant	1–4, varies for each building
PGA_j	Peak ground acceleration at building j location	Model response	—
T	Time span	Constant	50 years
v_j	Increase in lateral strength of building j due to retrofit	Decision variable	0
V_j	Building j base shear coefficient	Random variable	$N(0.12, 0.012)$
V_s	Shear wave velocity	Random variable	$U(760, 1,500)$ in meters per second for Site Class B per ASCE (2010)
E	Intraevent intensity model error	Random variable	$N(0, 1)$
ε_c	Cost model error	Random variable	$N(1, 0.1)$
ε_d	Damage model error	Random variable	$N(0, \sigma_{ed})$
ε_r	Retrofit cost model error	Random variable	$N(0, \sigma_{er})$
H	Interevent intensity model error	Random variable	$N(0, 1)$
η_j	Building j damage ratio	Model response	—
θ_d	Vector of damage model parameters	Random variable	Six normal random variables per Talebiyan (2016)
θ_r	Vector of retrofit cost model parameters	Random variable	Three normal random variables per Talebiyan (2016)
θ_{mi}	Source i magnitude uncertainty	Random variable	$N(0, 1)$
θ_{Li}	Source i location uncertainty	Random variable	$U(0, 1)$
λ_i	Source i occurrence rate	Constant	Value according to Table 3
σ_{ed}	Standard deviation of retrofit cost model error	Random variable	Normal random variable per Talebiyan (2016)
σ_{er}	Standard deviation of damage model error	Random variable	Normal random variable per Talebiyan (2016)

Note: $N(\mu, \sigma)$ and $LN(\mu, \sigma)$ denote normal and lognormal distributions with mean μ and standard deviation σ , respectively; $U(a, b)$ denotes a uniform distribution between a and b .

Table 3. Seismicity Parameters of Seismic Sources

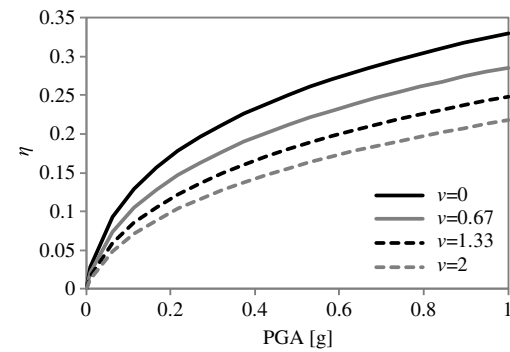
Source	M^{\max}		b'		λ (per year)
	Mean	Standard deviation	Mean	Standard deviation	
1	6.61	1.11	1.7420	0.2090	0.0357
2	7.64	1.02	1.3520	0.0010	0.0268
3	8.23	0.62	1.5760	0.0883	0.0712
4	6.02	0.54	1.2260	0.3310	0.0803
5	7.73	0.95	1.6660	0.1016	0.0357
6	7.17	0.83	0.7450	0.1565	0.0624
7	8.09	0.75	0.4620	0.0010	0.0178
8	7.72	0.98	1.5270	0.0010	0.0445
9	7.77	0.96	3.6620	0.0010	0.0268
10	5.40	0.48	1.6420	0.4483	0.0357
11	6.84	0.90	2.8290	0.3763	0.0891
12	6.79	0.86	0.6440	0.0753	0.0357
13	8.09	0.70	1.5000	0.1125	0.0982
14	8.06	0.30	1.3410	0.1140	0.2675
15	7.82	0.75	1.9920	0.2311	0.1336

and retrofit cost models. This approach relies both on mechanics and observed data. Using this approach enables the models to explicitly account for the uncertainty in the model parameters and the model error. In effect, Bayesian regression analysis determines the probability distribution of model parameters, which was updated as new data emerge. The general model form in this approach was

$$y = \theta_1 \cdot h_1(\mathbf{x}) + \theta_2 \cdot h_2(\mathbf{x}) + \dots + \theta_i \cdot h_i(\mathbf{x}) + \varepsilon \quad (19)$$

where y = model response; ϑ_i = model parameters; $h_i(\mathbf{x})$ = explanatory variables; and ε = model error. The ϑ parameters are random variables whose distributions are obtained from the Bayesian linear regression analysis. The model error is a normal random variable with a zero mean and a standard deviation of σ_ε . The latter is another random variable whose properties are determined by the Bayesian regression. In contrast, the explanatory variables of the model are determined by the mechanics of the problem. In the damage model, for instance, these are the variables that are deemed to affect the damage of buildings subject to earthquake. The damage model, repair cost model, and retrofit cost models are briefly introduced in the following.

Damage and repair cost models predict the seismic damage due to earthquake and its ensuing repair cost for a single building based on the characteristics of the building and the seismic intensity. The damage model predicts a damage ratio, defined as the cost of repairing the structural and nonstructural components divided by the cost of replacing the building. To conduct the regression analysis, damage ratios were generated for various sets of building characteristic and at different intensities using damage fragility curves proposed by Rota et al. (2008). These curves were developed based on the damage observed in 130,000 buildings that had been surveyed after earthquakes in Italy over three decades. These curves were chosen in this study because Italian masonry construction is similar to that of Iran. The data points employed to develop the damage model were extracted from these curves. Each data point includes plan irregularity, floor flexibility, number of stories, height, fundamental period, masonry type, PGA, base shear coefficient, and damage ratio [see Talebian (2016) for further details]. Based on this data set, 22 candidate model forms were developed and examined in terms of the prediction quality, heteroscedasticity, and normality of errors. Consequently, the functional form that best describes the data is known to be

**Fig. 5.** Damage ratio versus PGA for different values of v for $M = 0$, $I_p = 1$, $D = 0$, $N_s = 1$, and $V = 0.3$

$$\Phi^{-1}(\eta) = \theta_1 \cdot M + \theta_2 \cdot I_p - \theta_3 \cdot D + \theta_4 \cdot N_s + \theta_5 \cdot \ln(\text{PGA}) - \theta_6 \cdot \Phi[(1 + v) \cdot V] + \varepsilon \quad (20)$$

where η = damage ratio; M = masonry type, which is zero for CM and unity for URM; I_p = plan irregularity, which is unity if the building has a nonrectangular plan and zero otherwise; D = diaphragm type, which is zero for flexible diaphragms and unity for the rigid ones; N_s = number of stories; v = increase in lateral strength due to retrofit; and V = base shear coefficient that represents the current lateral strength. In fact, $v = 0$ indicates the current state of the building, while $v = 1$ means a 100% increase in the lateral strength. As mentioned previously, the characteristics of the ϑ parameters and model error, ε , are determined by Bayesian regression. Talebian (2016) gives the second moment information of these parameters, including mean, standard deviation, and correlation coefficient.

As Eq. (20) shows, the model correctly captured the increase in damage with PGA through the positive sign of ϑ_5 , and the reduction in damage with the building strength, $(1 + v) \cdot V$, through the negative sign of ϑ_6 . Hence, the damage and the ensuing repair cost was reduced by increasing v , i.e., strengthening the building through retrofit. These trends are illustrated in Fig. 5, which depicts the mean damage ratio predicted by Eq. (20) against PGA for different values of v . Given the damage ratio, repair cost is readily computed as follows:

$$c_l = \eta \cdot c_r \cdot A \cdot \varepsilon_c \quad (21)$$

where c_r = replacement cost per unit area; A = total floor area; and ε_c = model error.

The other group of model addressed here are the retrofit cost models. In a significant effort, a database of real-world data was compiled in this study to calibrate these models. In particular, the cost information of 98 retrofit projects on masonry school buildings in Iran were collected. For each building, the cost of applying shotcrete to strengthen the building along with the characteristics of the building were recorded. This method of retrofit entails anchoring a mesh of steel wires to the masonry wall followed by covering it with a thin layer of concrete. Among 46 candidate models that were inspected for prediction quality, heteroscedasticity, and normality of errors, the functional form that best describes the observations is

$$\ln(c_a/c_c) = -\theta_1 + \theta_2 \cdot A - \theta_3 \cdot D + \theta_4 \cdot M - \theta_5 \cdot c_c + \theta_6 \cdot \tan^{-1}(v) + \varepsilon \quad (22)$$

where c_a = retrofit cost per unit area; and c_c = initial construction cost per unit area. The normalization of c_a to c_c eliminates the need

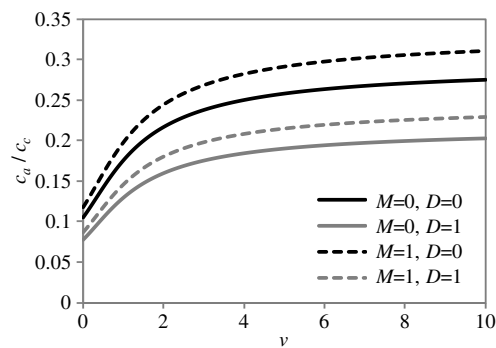


Fig. 6. Retrofit cost versus the increase in the lateral strength, v , for different values of masonry types, M , and diaphragm types, D

to develop different models for different geographical locations because that dependency is captured by c_c . Compared with models in the literature (FEMA 1994; Hopkins and Stuart 2003; Jafarzadeh et al. 2014; Potangaroa 1985), this model has the advantage of predicting the retrofit cost for a given level of retrofit v , and accounts for model uncertainty through the randomness of model parameters. Given $\ln(c_a/c_c)$, the total retrofit cost, c_o , is computed by

$$c_o = \exp[\ln(c_a/c_c)] \cdot c_c \cdot A \cdot \varepsilon_c \quad (23)$$

Fig. 6 depicts the ratio of mean c_a/c_c versus v for different types of masonry structures and diaphragm rigidities. As seen, the retrofit cost has an intercept, i.e., a fixed cost, that is mainly the cost of mobilization and setting up the construction site, among other things. Moreover, Fig. 6 shows that URM structures are more expensive to retrofit than CM structures, which is logical because URMs lack any confining element while CMs include tie beams and tie columns. Furthermore, Fig. 6 indicates that structures with flexible diaphragms need more investment for the same level of retrofit than those with rigid diaphragms. This is because of the superior seismic performance of rigid diaphragms in masonry structures compared with the flexible ones.

According to Fig. 6, the model correctly captures the increase in retrofit cost with v , as indicated by the positive sign of ∂_6 in Eq. (22). On the other hand, increasing v reduces the damage and ensuing repair costs, as was previously seen in the repair cost model. This reduction is, in fact, the return of the investment on retrofit. The idea behind the proposed methodology is to prioritize the buildings that yield a greater return per dollar investment.

Each of the 114 buildings in this study was modeled with a damage model, a repair cost model, and a retrofit cost model that was presented previously. A total of 1,142 model instances, 424 random variables, and 114 decision variables, collected in vector \mathbf{v} , were employed in this study. As described previously, Fig. 4 shows the flow of information between the models. These models are implemented in *Rt*, which is a computer program for multimodel reliability and optimization analysis. *Rt* was developed by Mahsuli and Haukaas (Mahsuli and Haukaas 2012; Mahsuli 2012), and is freely available online. The object-oriented architecture of *Rt* facilitates the steady growth of its probabilistic model library and analysis tools.

Portfolio Risk Analysis Results

This section presents the results of risk analysis on the portfolio of 114 school buildings in this study. Fig. 7 shows the cost exceedance probability curve that is computed in the current state of buildings denoted by $\mathbf{v} = \mathbf{0}$, i.e., when no retrofit is made. The time period T

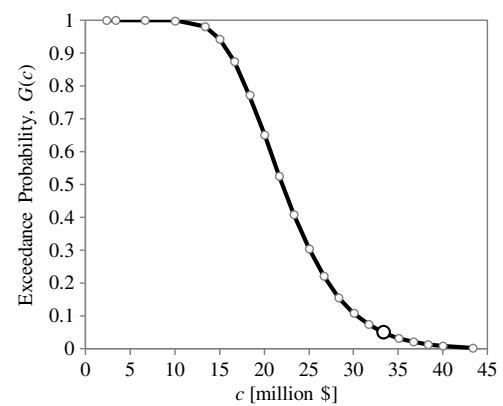


Fig. 7. Cost exceedance probability curve for the portfolio of 114 school buildings

was set to 50 years. As a result, c in the abscissa represents the maximum repair cost of the entire portfolio over the next 50 years. To put the costs into perspective, the mean total replacement cost of the portfolio is estimated at \$76 million. The ordinate in Fig. 7 presents the exceedance probability of cost, $G(c)$. The hollow circles in Fig. 7 illustrate the cost thresholds, i.e., c_t in Eq. (1), for which the load combination analysis was conducted. For instance, the probability of exceeding $c_t = \$33$ million over the next 50 years is 0.05. This cost threshold is equal to 44% of the mean portfolio replacement cost and is highlighted in Fig. 7 by a relatively larger hollow circle.

Prioritization Results

In this section, the 114 school buildings in central Iran are ranked for seismic retrofit in accordance with the proposed methodology. For this purpose, the sensitivity measure $1 - \partial E[c]/\partial c_{oj}$ was computed for each building in its current state. Fig. 8 illustrates this sensitivity measure as a bar at the location of each building. Each bar is depicted and colored based on the relative values of the said sensitivity measure. The legend in the figure provides the sensitivity value associated with each color. The higher and darker the bar, the more critical is the building for retrofit.

The top 10 buildings along with their respective sensitivity measures are presented in Table 4. As seen, all values of $1 - \partial E[c]/\partial c_{oj}$ are greater than zero because according to the per unit money spent on retrofit, there will be some savings due to the reduction of the repair cost. Table 4 also shows that even for buildings with the highest priority, the value of $1 - \partial E[c]/\partial c_{oj}$ is less than unity, meaning the investment is not fully returned. This value would go beyond unity if more consequences, such as casualties and downtime, were modeled. In this case, spending on retrofit would bring about a greater reduction of losses because of fewer casualties and shorter downtimes.

Fig. 3 locates the top 10 buildings on the map. It shows that they are mostly located in the northern part of the region. This is because the seismic sources are mainly located on the north of this region as demonstrated in Fig. 2. Therefore, the buildings in the north experience the highest earthquakes intensities, which bring about severe damages.

Table 4 helps to understand the characteristics of the prioritized buildings. The table shows that all of the top 10 buildings are URM and have flexible diaphragms. This trend is conspicuously seen across the entire portfolio in Fig. 9, which illustrates the sensitivities versus the rank for all buildings. Different colors in Fig. 9(a)

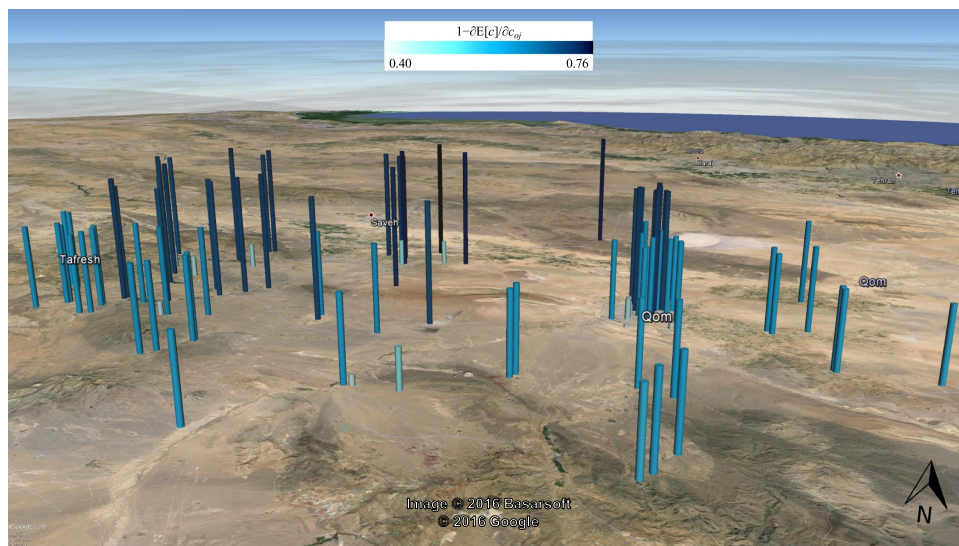


Fig. 8. Ranking of the 114 school buildings in central Iran for seismic retrofit using mean cost sensitivities (image © 2016 Basarsoft; © 2016 Google)

Table 4. Top 10 Prioritized Buildings Based on Mean Cost Sensitivities

Rank	Building	Footprint area (m ²)	Number of stories	Masonry type	Diaphragm type	$1 - \partial E[c]/\partial c_{oj}$
1	101	84	1	URM	Flexible	0.759
2	2	59	1	URM	Flexible	0.757
3	115	52	1	URM	Flexible	0.756
4	112	127	1	URM	Flexible	0.750
5	5	60	1	URM	Flexible	0.740
6	62	260	3	URM	Flexible	0.738
7	98	87	1	URM	Flexible	0.737
8	63	285	3	URM	Flexible	0.731
9	93	375	1	URM	Flexible	0.731
10	102	386	1	URM	Flexible	0.730

indicate different masonry types, and in Fig. 9(b) they indicate different diaphragm types. As seen in Fig. 9(a), URMs have a higher priority for retrofit. The same observation is made for structures with flexible diaphragms in Fig. 9(b). These observations are in agreement with the expectation that URM buildings, as well as the ones with flexible diaphragms, are generally more vulnerable, and thus take precedence in retrofit schemes.

Fig. 9(c) depicts sensitivities versus ranks in the same format but in different colors that represent the buildings in the following three regions: Qom City, Qom Suburbs, and Markazi Province. The figure shows that none of the regions dominate the top priorities. It suggests that there should be no preference between regions for the allocation of the retrofit budget. The reason is that these regions have similar construction methods and similar suppliers of construction materials due to their close proximity.

In addition to the mean cost sensitivity that provides a basis for risk-neutral ranking of the buildings, sensitivities of the higher moments of cost probability distribution were suggested for prioritization under risk-aversion. The ranking of the portfolio is expected to change when the attitude toward decision making alters. Figs. 10(a and b) show the ranking of all buildings based on $1 - \partial E[c]/\partial c_{oj}$ in the abscissa versus the ranking based on $1 - \partial(\sqrt{E[c^2]})/\partial c_{oj}$ and $\partial(E[c^5])^{1/5}/\partial c_{oj}$ in the ordinate, respectively. The figures indicate that the change in the risk attitude of the decision maker indeed modifies the ranking. The variation of the ranking is slight between the first and the second moments, and

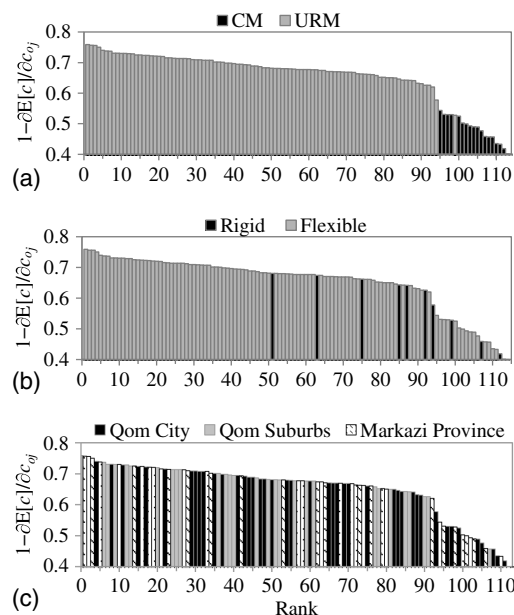


Fig. 9. Comparison of the mean cost sensitivities versus the rank of buildings between (a) URMs and CMs; (b) flexible and rigid diaphragms; (c) different regions

significant between the first and the fifth moments. The variation arises for buildings whose cost probability distribution has a heavy upper tail, i.e., buildings with a significant probability density for high costs. For such buildings, higher moments of cost distribution yield a significant risk measure, and consequently elevate the position of the building in the ranking. As a result, a risk-averse decision maker ensures that these buildings remain a high priority for retrofit and avoids confronting high losses in the aftermath of an impending earthquake. The more risk-averse the decision maker is, the higher is the chance that such buildings are promoted in the ranking. The order of the statistical moment to be used is determined by the degree of risk aversion of the decision maker, for instance, through the notion of the “basic reference lottery ticket question” (Jordaan 2005).

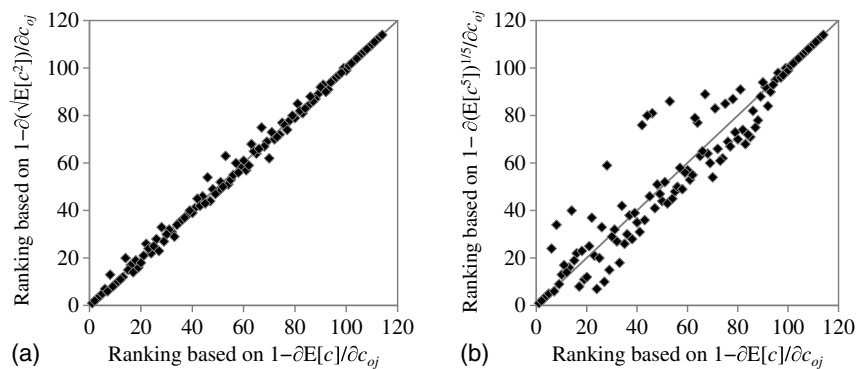


Fig. 10. Comparison of rankings based on the sensitivity of the mean cost versus the sensitivity of (a) the second moment; (b) the fifth moment of the probability distribution of cost

Concluding Remarks

This paper employed reliability and sensitivity analysis methods to address the all-important problem of allocating limited resources for regional risk mitigation. For optimal resource allocation, a portfolio of buildings within the region must be prioritized for seismic retrofit. The rationale behind the proposed solution is that investment must be made where the most return is expected, which here translates to the most reduction in the regional loss per dollar spent on the retrofit of each building. A dimensionless sensitivity measure was formulated using the derivative of the expected regional cost with respect to the retrofit cost of each building. This measure reveals the rate of savings in the repair costs of the entire portfolio when each building is retrofitted. To provide flexibility for prioritization under risk aversion, measures for the sensitivity of higher moments of the regional cost probability distribution were proposed. Thereafter, the effect of the degree of risk aversion on the prioritization was studied. This paper employed direct differentiation method to derive closed-form relationships of the proposed sensitivity measures. The proposed measures were showcased in a comprehensive application to prioritize a portfolio of 114 masonry school buildings in Iran for seismic retrofit. To conduct such an analysis, new models were developed for probabilistic prediction of the seismic repair cost and retrofit cost of masonry buildings that were calibrated to observed data. The resulting rankings gave unreinforced masonry buildings precedence over confined masonry buildings. Also, structures with flexible diaphragms were prioritized over the ones with rigid diaphragms. The results are in line with observations in past earthquakes owing to the fact that the underlying cost models were calibrated to such observations.

The proposed sensitivity measures have the potential to address more complex problems. For instance, they can be developed to prioritize the components of any infrastructure for rehabilitation. The measures are also capable of accounting for any interdependencies between infrastructure components because they are based on the total infrastructure cost. Hence, the fact that rehabilitating a single component may enhance the performance of other interdependent components is captured by these measures. Finally, the derivation of the sensitivities in this paper features multiple hazards and their possible coincidence, which provides them with the potential to address multihazard problems, e.g., when the infrastructure is subject to earthquakes, floods, hurricanes, and so on in its lifetime.

Acknowledgments

The financial support of Sharif University of Technology through Grant No. G930930 is gratefully acknowledged. The authors thank

the collaboration of the State Organization of School Renovation in providing access to the records of seismic retrofit plans for school structures. In particular, the authors gratefully thank Mr. Arash Mardani, Director of Research, for valuable cooperation and discussion throughout the course of this research. Finally, the authors express their gratitude to Messrs. Hossein Nasr Azadani and Hamid Etebarian for collaboration in data collection.

References

- Artzner, P., Delbaen, F., Eber, J. M., and Heath, D. (1999). "Coherent measures of risk." *Math. Finance*, 9(3), 203–228.
- ASCE. (2010). "Minimum design loads for buildings and other structures." *ASCE/SEI 7-10*, Reston, VA.
- Bernoulli, D. (1738). "Exposition of a new theory on the measurement of risk." *Econometrica*, 22(1), 23–36.
- Bonstrom, H., and Corotis, R. B. (2015). "Optimising portfolio loss reduction using a first-order reliability method sensitivity analysis." *Struct. Infrastruct. Eng.*, 11(9), 1190–1198.
- Box, G. E. P., and Tiao, G. C. (1973). *Bayesian inference in statistical analysis*, Addison-Wesley, Boston.
- Der Kiureghian, A. (2005). "First- and second-order reliability methods." *Engineering design reliability handbook*, E. Nikolaidis, D. Ghiocel, and S. Singhal, eds., CRC Press, Boca Raton, FL.
- Der Kiureghian, A., Ditlevsen, O. D., and Song, J. (2007). "Availability, reliability and downtime of systems with repairable components." *Reliab. Eng. Syst. Saf.*, 92(2), 231–242.
- FEMA. (1988). "Rapid visual screening of buildings for potential seismic hazards: A handbook." *FEMA 154*, Applied Technology Council, Redwood City, CA.
- FEMA. (1994). "Typical costs for seismic rehabilitation of existing buildings. V1: Summary." *FEMA 156*, Washington, DC.
- Gardoni, P., Der Kiureghian, A., and Mosalam, K. M. (2002). "Probabilistic capacity models and fragility estimates for reinforced concrete columns based on experimental observations." *J. Eng. Mech.*, 10.1061/(ASCE)0733-9399(2002)128:10(1024), 1024–1038.
- Grant, D. N., Bommer, J. J., Pinho, R., Calvi, G. M., Goretti, A., and Meroni, F. (2007). "A prioritization scheme for seismic intervention in school buildings in Italy." *Earthquake Spectra*, 23(2), 291–314.
- Gutenberg, B., and Richter, C. F. (1944). "Frequency of earthquakes in California." *Bull. Seismol. Soc. Am.*, 34(4), 185–188.
- Hopkins, D. C., and Stuart, G. (2003). "Strengthening existing New Zealand buildings for earthquake: An analysis of cost benefit using annual probabilities." *Pacific Conf. on Earthquake Engineering*, New Zealand Society for Earthquake Engineering, New Zealand.
- Jafarzadeh, R., Ingham, J. M., Walsh, K. Q., Hassani, N., and Ghodrati Amiri, G. R. (2014). "Using statistical regression analysis to establish construction cost models for seismic retrofit of confined masonry buildings." *J. Constr. Eng. Manage.*, 10.1061/(ASCE)CO.1943-7862.0000968, 04014098.

- Jordaan, I. (2005). *Decisions under uncertainty: Probabilistic analysis for engineering decisions*, Cambridge University Press, Cambridge, U.K.
- Kaklamanos, J., Boore, D. M., Thompson, E. M., and Campbell, K. W. (2010). "Implementation of the next generation attenuation (NGA) ground-motion prediction equations in Fortran and R." *Open-File Rep. 2010-1296*, USGS, Washington, DC.
- Mahsuli, M. (2012). "Probabilistic models, methods, and software for evaluating risk to civil infrastructure." Ph.D. dissertation, Univ. of British Columbia, Vancouver, Canada.
- Mahsuli, M., and Haukaas, T. (2012). "Computer program for multimodel reliability and optimization analysis." *J. Comput. Civ. Eng.*, **10.1061/(ASCE)CP.1943-5487.0000204**, 87–98.
- Mahsuli, M., and Haukaas, T. (2013a). "Seismic risk analysis with reliability methods. Part I: Models." *Struct. Saf.*, **42**, 54–62.
- Mahsuli, M., and Haukaas, T. (2013b). "Seismic risk analysis with reliability methods. Part II: Analysis." *Struct. Saf.*, **42**, 63–74.
- Mahsuli, M., and Haukaas, T. (2013c). "Sensitivity measures for optimal mitigation of risk and reduction of model uncertainty." *Reliab. Eng. Syst. Saf.*, **117**, 9–20.
- Monti, G., and Nuti, C. (1996). "A procedure for assessing the functional reliability of hospital systems." *Struct. Saf.*, **18**(4), 277–292.
- Nuti, C., Santini, S., and Vanzi, I. (2004). "Damage, vulnerability and retrofitting strategies for the Molise hospital system following the 2002 Molise, Italy, earthquake." *Earthquake Spectra*, **20**(S1), S285–S299.
- Nuti, C., and Vanzi, I. (1998). "Assessment of post-earthquake availability of hospital system and upgrading strategies." *Earthquake Eng. Struct. Dyn.*, **27**(12), 1403–1423.
- Potangaroa, R. (1985). "The seismic strengthening of existing buildings for earthquakes." Master's thesis, Victoria Univ., Wellington, New Zealand.
- Power, M., Chiou, B., Abrahamson, N., Bozorgnia, Y., Shantz, T., and Roblee, C. (2008). "An overview of the NGA project." *Earthquake Spectra*, **24**(1), 3–21.
- Rahimi, H., Mahsuli, M., and Bakhshi, A. (2015). "Reliability-based seismic hazard analysis." *12th Int. Conf. on Applications of Statistics and Probability in Civil Engineering*, Univ. of British Columbia, Vancouver, Canada.
- Rockafellar, R. T. (2007). "Coherent approaches to risk in optimization under uncertainty." *Tutorials in operations research*, Vol. 3, Institute for Operations Research and the Management Sciences, Catonsville, MD, 38–61.
- Rota, M., Penna, A., and Strobbia, C. L. (2008). "Processing Italian damage data to derive typological fragility curves." *Soil Dyn. Earthquake Eng.*, **28**(10–11), 933–947.
- Rt [Computer software]. Univ. of British Columbia, Vancouver, Canada.
- Talebiyan, H. (2016). "Optimal seismic risk mitigation by prioritization of structures for retrofit." Master's thesis, Sharif Univ. of Technology, Tehran, Iran.
- Tesfamariam, S., and Saatcioglu, M. (2008). "Risk-based seismic evaluation of reinforced concrete buildings." *Earthquake Spectra*, **24**(3), 795–821.
- Vanzi, I. (2000). "Structural upgrading strategy for electric power networks under seismic action." *Earthquake Eng. Struct. Dyn.*, **29**(7), 1053–1073.
- von Neumann, J., and Morgenstern, O. (1944). *Theory of games and economic behavior*, Princeton University Press, Princeton, NJ.
- Wen, Y. K. (1990). *Structural load modelling and combination for performance and safety evaluation*, Elsevier, Amsterdam, Netherlands.